# Cessna Citation X Business Aircraft Eigenvalue Stability– Part 1: a New GUI for the LFRs Generation

Yamina BOUGHARI[1], Ruxandra Mihaela BOTEZ*[,1], Florian THEEL[1], Georges GHAZI[1]

*Corresponding author
[1]ETS, Laboratory of Active Controls, Avionics and AeroServoElasticity LARCASE, 1100 Notre Dame West, Montreal, Que., Canada, H3C-1K3,
yamina.boughari.1@ens.etsmtl.ca, Ruxandra.Botez@etsmtl.ca*, f.theel@gmail.com, georges.ghazi.1@ens.etsmtl.ca

DOI: 10.13111/2066-8201.2017.9.4.4

*Received: 21 October 2017/ Accepted: 07 November 2017/ Published: December 2017*


**Abstract:** *The aim of "Robustness Analysis" is to assess aircraft stability in the presence of all admissible uncertainties. Models that are able to describe the aircraft dynamics by taking into account all uncertainties over a region inside the flight envelope have therefore been developed, using Linear Fractional Representation (LFR). In this paper Part 1 a friendly Graphical User Interface is developed to facilitate the generation of Linear Fractional Representation uncertainty models for the Cessna Citation X aircraft using 12 weight and Xcg configurations; thus, 26 regions of the flight envelope are developed for different Weight/ Xcg configurations to study the aircraft's longitudinal motion. In the aim to analyzed the robustness stability of Cessna Citation X in Part 2 using the Graphical User Interface developed in the Clearance Of Flight Control Laws Using Optimization (COFCLUO) project. This project aimed to boost the aircraft safety using computer computation*.

***Key Words****: Linear Fractional Representation; Flight Control Clearance; Stability Analysis Robustness Analysis*

## NOMENCLATURE

| | |
|---|---|
| *X*, *Z* | = Aircraft aerodynamic forces |
| $x(t)$ | = State space parameter of the system |
| $\theta$ | = Pitch angle |
| *u*, *w* | = Speeds along the *Ox*, *Oz* axes |
| *q* | = Angular speed along the *Ox* axes |
| *V* | = Total Aircraft Speed |
| $\delta_e$ | = Elevator deflections |
| $\Delta$ | = Block uncertainties |
| *V(x)* | = System energy |
| *A*, *B*, *C*, *D* | =State space matrices |

## 1. INTRODUCTION

In any aircraft design process, the Flight Control Laws (FCL) have to be cleared, qualified, and certified [1]. A simulation technique involving a flight envelope expressed by grid of points was used; for each grid point the model simulation verified if the specifications were satisfied or not [2]. The main disadvantages of this technique were two-fold: first, the local results were obtained following a partial study [1], and therefore, despite a significant density of the number of points, it was always possible to neglect the most critical flight cases. And secondly, the technique's execution time depended directly on the required accuracy, and therefore on the grid refinement. However, due to the execution time involved and the considerable design cost, analyzing a full flight envelope model was not possible with the existing team computer capabilities as the number of cases contained within the flight envelope and the weight/Xcg configurations, were very high.

To enable the use of rapid, comprehensive and effective analysis methods, parameter-varying models have been developed by incorporating variations, (also known as "uncertainties" in their nominal models). These models were built for several flying conditions, by use of a parametric method called Linear Fractional Transformation (LFT) [3]-[7]. The use of such a method has gained the attention of aeronautical companies. Results were provided which indicated to the industry that there was a promising future for the modeling of control laws' design and certification [8], and it was expected to reduce the number of required flight maneuvers [9].

Several methods were investigated with the aim to generate of the LFT parametric models ([10]-[13]). LFT is based primarily on the number of different types of uncertainties that are incorporated in the aircraft dynamic model. For example, a multiplicative parametric uncertainty was considered for a robust Gust Load Alleviation of B-52 aircraft, and analyzed using *mu -synthesis* [14]. One of the two forms of uncertainties: "unknown (or unstructured) uncertainty" structure, and well-defined, known as "structured uncertainties" could be chosen. These types of uncertainties have been investigated for the stabilization problems, and were further illustrated for the thrust vectoring aircraft [15]. The LFT method represents one of the more challenging methods for the incorporation of aerodynamic uncertainties [16]-[17] or of the Xcg, mass and inertia variations in the aircraft model. Several approaches for obtaining a very good quality and a reduced order of LFT models have been investigated based on the number and complexity of parametric uncertainties [18]-[19].

In the flight clearance process, an aircraft system with parameter uncertainties has been transformed into LFR model by using LFT, as shown in [20], where a robustness analysis was performed on an unmanned helicopter flight using *mu-analysis*. In [21], the *H-infinity* control method was used for the flight clearance of a longitudinal aircraft model having parametric uncertainties. In [22] both *H-infinity* and *mu-analysis* were investigated for the robust control of flexure joint struts of Stewart Platform.

Our current research focuses on the Cessna Citation X open loop stability analysis. The data are provided by a Level D Research Aircraft Flight Simulator (RAFS), where Level D corresponds to the highest level flight dynamics certification by the FAA. The RAFS was designed and manufactured by CAE Inc. for the research purposes of the LARCASE team at the ETS. These data were used to develop both nonlinear and linear models of the airplane for its longitudinal and lateral motions [23], [24], where optimal, and *H-infinity* controllers were designed using meta-heuristic algorithms [25]- 29], and cleared for the Cessna Citation flight envelope using [30]. In addition, 26 longitudinal LFR models were created for 12 Xcg and weight configurations of the whole flight envelope. A user-friendly GUI was developed during this study to automate the LFR model generation. The LFR models were further analyzed in article Part2 using the robustness and stability analysis toolbox to assess the Cessna Citation X aircraft eigenvalue stability.

The paper is organized as follows: Firstly, a presentation of the Cessna Citation X aircraft. Next, a description of the Linear Fractional Representation (LFR) method is given, and the paper ends with the LFR toolbox, the LFR validation results, and conclusions.

## 2. CESSNA CITATION X BUSINESS AIRCRAFT

The Cessna Citation X operates at a Mach number of 0.935; thus, it is the fastest civilian aircraft in the world. The nonlinear model for the development and validation of this aircraft's flight control system uses the Cessna Citation X's flight dynamics that is detailed in [28]. This model was built in Matlab/Simulink, and is based on aerodynamics data extracted from a Cessna Citation X Level D Research Aircraft Flight Simulator designed and manufactured by CAE Inc. According to the Federal Administration Aviation (FAA, AC 120-40B), Level D is the highest certification level that can be delivered by the Certification Authorities for an aircraft's flight dynamics. More than 100 flight tests were performed on the Citation X Level D Research Aircraft Flight Simulator within its aircraft flight envelope, for the research presented in this paper.

Using trim and linearization routines developed in [23], [24], the aircraft longitudinal and lateral equations of motions were linearized for various flight conditions expressed in terms of altitudes and speeds, and for different aircraft configurations in terms of mass and center of gravity positions. In order to validate these different models obtained by this linearization, several comparisons of them with the linear model obtained using the identification techniques proposed in ([31], [32]) were performed for different flight conditions and aircraft configurations.

The results have shown that the linear models were accurate and could be further used to estimate the local behavior of the Cessna Citation X for any flight condition.

The linearized aircraft equations of motion are represented in the form of the following state space system [24], and [33]:

$$\dot{x} = \mathrm{A}x + \mathrm{B}u \tag{1}$$

This system is decomposed into two sub-systems representing the aircraft's longitudinal and lateral motions.

Only the aircraft's longitudinal motion dynamics are considered for the stability, and are given by the state space equation, using the elevator deflections as input:

$$\dot{x}_{\mathrm{long}} = \mathrm{A}_{\mathrm{long}} x_{long} + \mathrm{B}_{\mathrm{long}} u_{long}$$

$$\mathrm{A}_{\mathrm{Long}} = \begin{pmatrix} \mathrm{X_u} & \mathrm{X_w} & \mathrm{X_q} & -\mathrm{g}\cos\theta \\ \mathrm{Z_u} & \mathrm{Z_w} & \mathrm{Z_q} & 0 \\ \mathrm{M_u} + \mathrm{M_{\dot{w}}}\mathrm{Z_u} & \mathrm{M_w} + \mathrm{M_{\dot{w}}}\mathrm{Z_w} & \mathrm{M_q} + \mathrm{M_{\dot{w}}}\mathrm{u_0} & 0 \\ 0 & 0 & 1 & 0 \end{pmatrix}, \mathrm{B}_{\mathrm{Long}} = \begin{pmatrix} \mathrm{X}_{\delta_e} \\ \mathrm{Z}_{\delta_e} \\ \mathrm{M}_{\delta_e} + \mathrm{M_{\dot{w}}}\mathrm{Z}_{\delta_e} \\ 0 \end{pmatrix} \tag{2}$$

where A represents the stability derivatives matrix, and B represents the control derivatives matrix; the state vector $x_{long}(t)$ and control vector $u_{long}(t)$ are given by eq.(3):

$$x_{long}(t) = (\mathrm{u} \quad \mathrm{w} \quad \mathrm{q} \quad \theta)^{\mathrm{T}} \text{ and } u_{long}(t) = \delta_{\mathrm{e}} \tag{3}$$

In [23] a linear model was obtained for 36 flight conditions for the Cessna Citation X business aircraft, that was based on data extracted from the Level D Research Aircraft Flight Simulator (RAFS) tests performed at the LARCASE laboratory [23]. The models used Linear Fractional Representation (LFR) that considered their uncertainties; LFR models were obtained using the bilinear interpolation method [34]-[36]. The following section offers a brief description of the LFR method, and its application on the Cessna Citation X model business aircraft.

## 3. LINEAR FRACTIONAL REPRESENTATION (LFR)

LFR changes a group of linearized models by means of their "progression". These linearized models are used to define "state matrices" by keeping a range of error known as "uncertainties" in their design. To define the robustness of the modeling of the system analysis, the uncertainties are extracted from the state matrices coefficients', and are arranged into a block named "Δ". This matrix "Δ" contains information about a model's fluctuations around its nominal value. The matrix is of an order at least equal to the sum of all the uncertainties' repetitiveness', where "repetitiveness" reflects when an uncertainty appears more than once in the expression of a matrix' coefficients. In addition, block Δ contains as many integrators as the order of the system. Figure 1 and Figure 2 illustrate an LFR model.

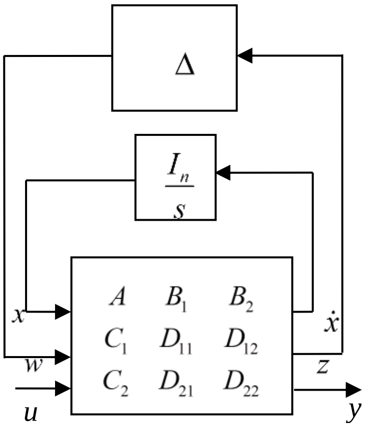


Figure 1. LFR of $K\left(\frac{1}{s}, \delta_1, \ldots, \delta_q\right)$ transfer function

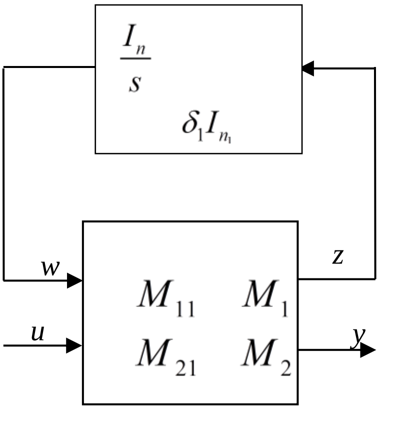


Figure 2. The LFR of Δ block

From Figure 2, eqs. (4)-(6) are obtained:

$$\dot{x} = Ax + B_1 w + B_2 u \tag{4}$$

$$z = C_1 x + D_{11} w + D_{12} u \tag{5}$$

$$y = C_2 x + D_{21} w + D_{22} u \tag{6}$$

where

$$w = \Delta u \quad \text{where} \quad \Delta = \text{Diag}\left(\delta_1 I_{n_1}, \dots, \delta_q I_{n_q}\right) \tag{7}$$

If the Linear Fractional Representations of the block Δ given by Figure 2 and Figure 3 are compared, we can deduce that:

$$M_{11} = \begin{bmatrix} A & B_1 \\ C_1 & D_{11} \end{bmatrix}; M_{12} = \begin{bmatrix} B_2 \\ D_{12} \end{bmatrix}; \quad M_{12} = [C_2 \quad C_{21}]; M_{22} = D_{22} \tag{8}$$

***Definition 2*** [34]:

*1. The Upper Linear Fractional Transformation LFT* $F_u(M, \Delta)$:

In Figure 2, the transfer function between *u* and *y* given by closing the loop of block Δ is denoted by $F_u(M, \Delta)$:

$$F_u(M, \Delta) = M_{21}\Delta(I - M_{11}\Delta)^{-1}M_{12} + M_{22} \tag{9}$$

where $M = \begin{bmatrix} M_{11} & M_{12} \\ M_{21} & M_{22} \end{bmatrix}$

*2. The Lower Linear Fractional Transformation LFT* $F_l(M, K)$:

After closing the loop using $y = Ku$, the transfer function is denoted as $F_l(M, K)$:

$$F_l(M, K) = M_{12}K\,(I - M_{22}K)^{-1}M_{21} + M_{11} \tag{10}$$

In order to facilitate the modeling and the use of LFR systems, a toolbox was developed by ONERA, which used Matlab® software that contained several useful features [35].

The uncertainties of Altitude and True Air Speed (TAS) are the crucial parameters required to obtain an LFR model for the Cessna Citation X business aircraft, and to build a system involving uncertainties covering its whole aircraft envelope. The aircraft model is linearized for an altitude range between 0 – 51,000 ft and a TAS range of 120-425 knots. A graphical representation of the Cessna Citation X linearized model flight points within its flight envelope is given in Figure 3.

There are several approaches used to generate LFR models by use of both "direct" and "indirect" methods. The methods commonly used in research to obtain such representation were discussed in [1].

In this paper, the LFR model based on interpolation is considered to be generated by a direct method; a database of linearized flight points is considered by using the *Trends and Bands* technique, that is illustrated in the next section.

### 3.1 LFR Modeling using Trends and Bands method

To perform a Linear Fractional Transformation (LFT), the first step is to determine how the state matrices describe an uncertain model changes according to the True Air Speed (TAS) and the altitude.

In the case of the Cessna Citation X aircraft, a set of linearized models expressed in the state space form, based on data extracted from the Research Aircraft Flight Simulator (RAFS) provided by CAE Inc. for different flight conditions using altitudes and TAS as variables (see Figure 3), are available for a set of weights and Xcg configurations, as shown in Figure 4. Matrices A and B can then be obtained for a fixed weights and Xcg configurations in the following form:

$$\text{A} = \text{A}(h, TAS) \tag{11}$$

$$\mathrm{B} = \mathrm{B}(h, TAS) \tag{12}$$

The aircraft dynamics is described for the flight envelope conditions. Figure 3 shows the 36 flight points selected within the flight envelope limits. The aircraft models are obtained at each 5000 ft in the flight envelope, for 4 different speeds.

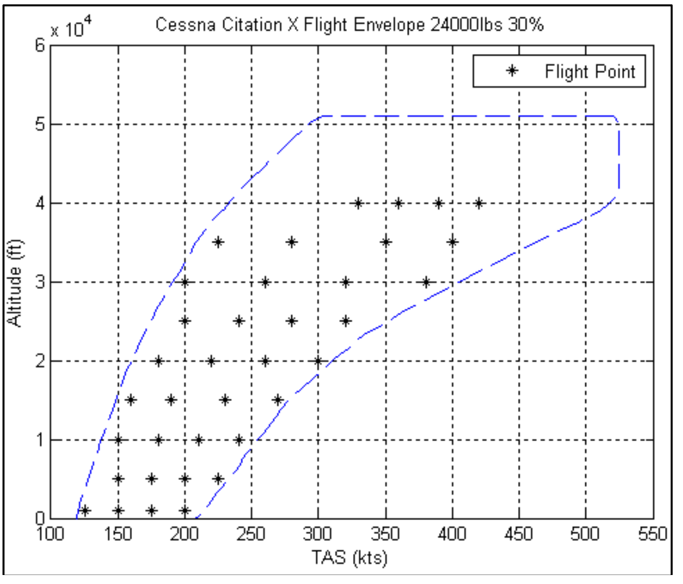


Figure 3. Cessna Citation X Aircraft Flight Envelope

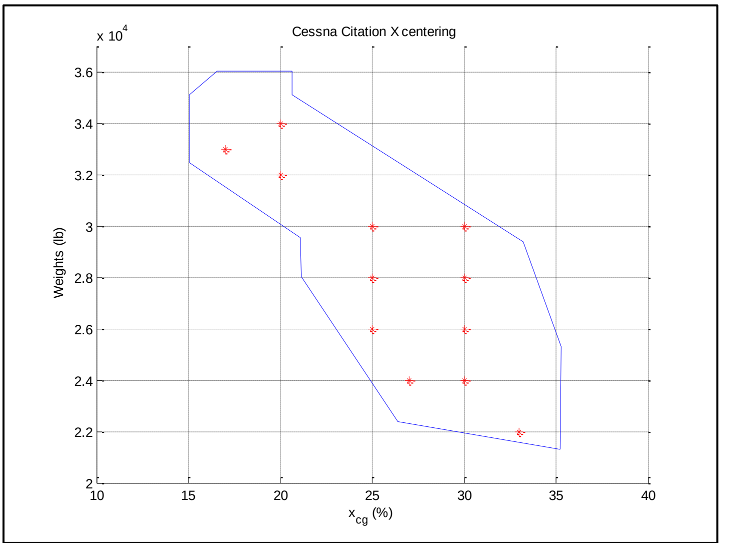


Figure 4. Cessna Citation X Weight/Xcg conditions

Before carrying out the interpolation, two steps must be performed. The first step defines the region for an altitude and a range of TAS where the interpolation will be performed; the four (4) corners of the region form the vertices as shown in Figure 5.

Each of the TAS ranges has a lower and an upper value, which are its bounds. The second step is the normalization of these bounds in order to attribute each coordinate of the vertices a value equal to 1 or -1.

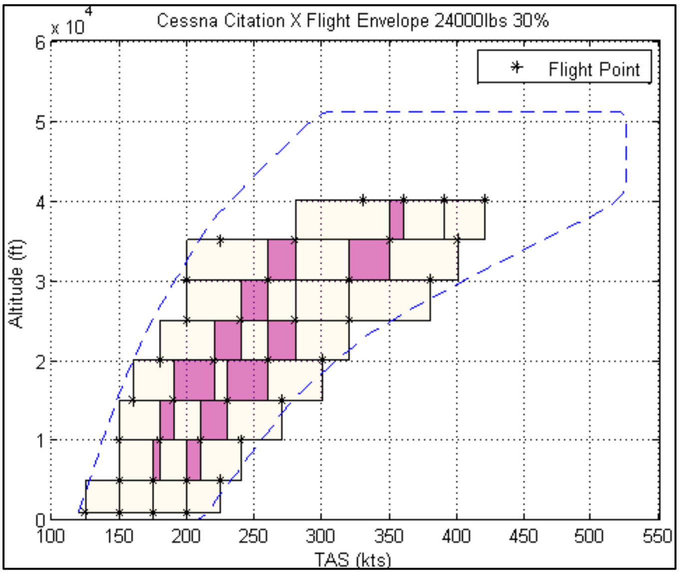


Figure 5. 26 Regions Definition

### 3.2 Normalization

The function used to proceed to the regions' normalization allows the "coordinates" of the two uncertainties parameters the TAS and the altitude to be associated with a pair of normalized coordinates in the variation range. Since each region has neither the same form nor the same limits, it was necessary to develop a generic code with the aim to adapt the different values taken by these regions.

Ideally, three vertices of the region are sufficient to normalize the concerned region; this normalization reduces the system of equations to a system of three equations with three unknowns for the two (2) uncertainties.

The minimum and maximum values, as well as the positions of the two vertices, diagonally opposite one to another were associated with these values. The third vertex position is selected as one of the two remaining vertices positions. The normalized values associated with these three positions are the following: $\{[-1;-1],[-1;1],[1;1]\}$ or $\{[-1;-1],[1;-1],[1;1]\}$.

The matrix form implementation of what is shown in equation (14), and allows the obtaining of the coefficients $a_i, b_i, c_i$ for each uncertainty, by allowing the uncertainty to be given by equation (13):

$$Inc_i = a_i + b_i\delta_1 + c_i\delta_2 \tag{13}$$

where $\delta_i \in [-1,1]$ , and $i = [1,2] \in N$

$$\begin{bmatrix} Inc_{i,1} \\ Inc_{i,2} \\ Inc_{i,3} \end{bmatrix} = \begin{bmatrix} 1 & -1 & -1 \\ 1 & -1 & 1 \\ 1 & 1 & 1 \end{bmatrix} \begin{bmatrix} a_i \\ b_i \\ c_i \end{bmatrix} \text{ or } \begin{bmatrix} Inc_{i,1} \\ Inc_{i,2} \\ Inc_{i,3} \end{bmatrix} = \begin{bmatrix} 1 & -1 & -1 \\ 1 & 1 & -1 \\ 1 & 1 & 1 \end{bmatrix} \begin{bmatrix} a_i \\ b_i \\ c_i \end{bmatrix} \tag{14}$$

Equation (13) has two varying terms ($\delta_1$, $\delta_2$), which are used to define the regions of rectangular or parallelogram shapes. Thus, it is easy to move from a normalized basis to a non-normalized basis and vice versa by inverting coefficients matrix in eq. (14). We note that this operation it is used to obtain the determinant of the matrix presented in eq. (15). The normalized coordinates for each point used for interpolation are determined from eq. (15), which is obtained under matrix form from eq. (13):

$$\begin{pmatrix} 1 \\ \delta_1 \\ \delta_2 \end{pmatrix} = \begin{pmatrix} 1 & 0 & 0 \\ a_1 & b_1 & c_1 \\ a_2 & b_2 & c_2 \end{pmatrix}^{-1} \begin{pmatrix} 1 \\ Inc_1 \\ Inc_2 \end{pmatrix} \tag{15}$$

Table 1 presents the coefficients values obtained from two regions' coordinates:

Table 1. Normalization Coefficients and Coordinates

| Classification of Interpolation Points (Step 1) "Reference points'' | Normalization of Coefficients $a_i$ $b_i$ $c_i$ (Step 2) | Normalization of Coordinates (Step 3) |
|---|---|---|
| Point 1: [125; 1000]<br>Point 2: [150; 1000]<br>Point 3: [150; 5000] | i=1, [137,5; 12,5 ; 0]<br>i=2, [3000 ; 0 ; 2000] | [-1; -1]<br>[1; - 1]<br>[1; 1] |
| Point 1: [200; 5000]<br>Point 2: [225; 5000]<br>Point 3: [240; 10000]<br>Point 4: [210; 10000] | i=1, [220; 20 ; 0]<br>i=2, [7500 ; 0; 2500] | [-1; -1]<br>[0.25; -1]<br>[1; 1]<br>[-0.5; 1] |

To optimize the accuracy of the results, the smallest possible regions have been defined, containing only 3 or 4 flight points to use as "reference points" for the interpolation. This definition allows performing a bilinear interpolation for which 4 coefficients must be found by using eqs. (16) - (18):

$$\mathrm{A}(h, TAS) = \mathrm{A}_{0_{4,4}} + \mathrm{A}_{1_{4,4}} h + \mathrm{A}_{2_{4,4}} TAS + \mathrm{A}_{3_{4,4}} TAS \times h \tag{16}$$

$$\mathrm{B}_{\mathrm{long}}(h, TAS) = \mathrm{B}_{0_{4,1}} + \mathrm{B}_{1_{4,1}} h + \mathrm{B}_{2_{4,1}} TAS + \mathrm{B}_{3_{4,1}} TAS \times h \tag{17}$$

$$\mathrm{B}_{\mathrm{lat}}(h, TAS) = \mathrm{B}_{0_{4,2}} + \mathrm{B}_{1_{4,2}} h + \mathrm{B}_{2_{4,2}} TAS + \mathrm{B}_{3_{4,2}} TAS \times h \tag{18}$$

The Least Square (LS) method is employed to minimize the relative errors in the "reference points". The maximum relative errors found for the state space matrices A and B coefficients are between $10^{-13}$ à $10^{-15}$, thus are neglected, and therefore these coefficients values are considered to be very good.

Using the reference points, which are the flight points obtained from the flight tests and shown in Figure 3, a number of 26 regions (rectangular) are reached, which cover a large part of the flight envelope expressed in terms of altitude and TAS. The region division is valid for all weight and balance conditions, and is presented in Figure 5. It can be observed from Figure 5 that some of the regions superimpose over other regions (darker zones) due to their common reference points; in many cases there is not only an interpolation applies but also extrapolation applies to obtain these regions.

The achievement of 26 models for 12 different Xcg/weight configurations takes 59.28 seconds by means of LFR, and takes 0.19 seconds by region. The computing time is acceptable following the usefulness of presented results. These models are calculated for regions shown in Figure 5.

The final phase of generating the LFR system is based on the last two steps: 1) obtaining the LFR system and 2) its minimization. Thus, four LFR systems are found that representing our four state space matrices (A,B,C,D), although the C and D matrices do not contain uncertainties. Next, an overall system is designed using the “abcd2lfr” command in Matlab® by specifying the states number which is equal to four. Information regarding the order of the system and the uncertainties’ repetitiveness are presented in the following Table 2 for the longitudinal aircraft model design. By using the “minlfr” function, the order of the system can be reduced from 24 to 13 when the region used 4 reference flight points for interpolation, and from 13 or 14 to 10 when the region used 3 reference flight points as shown in Table 2.

Table 2. LFR’s system order and repetitiveness

| | Longitudinal LFR models | |
|---|---|---|
| Number of reference points used in the interpolation | 3 | 4 |
| System order | 13 or 14 | 24 |
| System order after minimization | 10 | 13 |
| TAS repetitiveness | 3 | 3 |
| Altitude repetitiveness | 3 | 6 |

A comparison of a full order LFR system with its reduced system results is shown in Figure 6 for a given weight/Xcg configuration, and for medium altitudes regions; results are shown for regions 15 to 18 in Figure 6, while for the other 22 regions results are given in the Appendix. This comparison demonstrates that the reduction of the system preserved its main characteristics, where the full-order LFR system poles (blue circles) are perfectly consistent with those of the reduced order LFR system poles (red crosses).

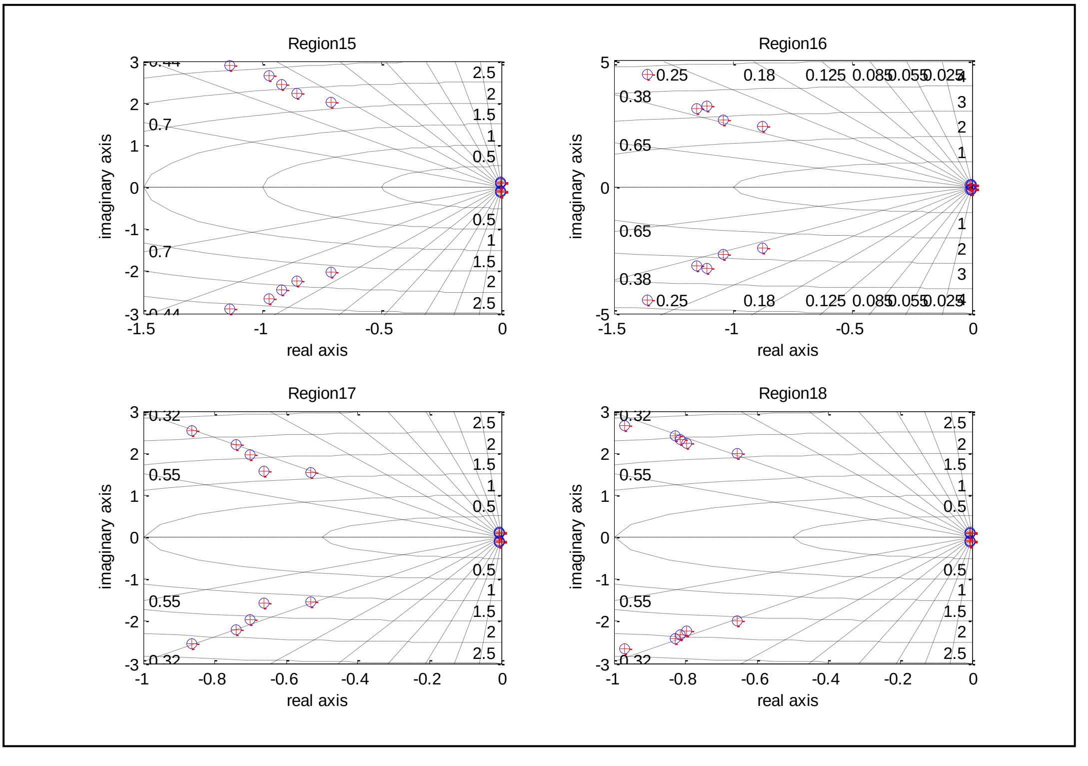


Figure 6. Full-order LFR system versus a reduced-order LFR system

To automate the Cessna Citation X aircraft's LFR model generation, and for a better visualization, a GUI was developed to encompass all these steps from the beginning of the research, and is presented in the next Section.

## 4. THE GRAPHICAL USER INTERFACE GUI

A user-friendly Graphical User Interface (GUI) was developed, showing the major steps for the generation of the LFR models, their reduction, and their validations. As shown in Figure 7, it is possible to determine the type of interpolation: bilinear or biquadratic, the type of model: lateral or longitudinal, the Xcg location terms, and the definition of the regions.

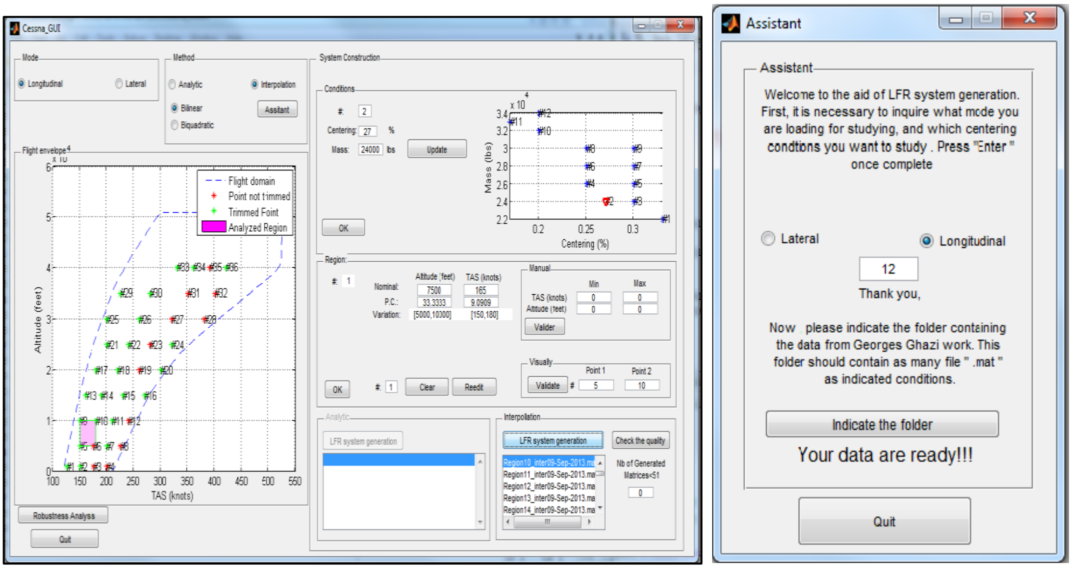


(a) (b)

Figure 7. Graphical User Interface for generating the Cessna Citation X LFRs.

To subdivide the flight envelope into regions, the following three ways are offered by using the GUI:

1. "Manually" -- by specifying "the upper and lower bounds of each uncertainty". The "Submit" button associated with the manual method must be chosen to show the nominal values and the percentage of the uncertainties, corresponding to each parameter (TAS and altitude). By clicking on "OK", the selected region appears in a colored square shape in the flight envelope, as shown in figure 7 (a).
2. "Visually" -- by specifying the "opposite diagonal vertices".
3. "Directly" -- by "filling the nominal value of each parameter and the percentage of uncertainties

Once all informations have been provided, the interface allows us to build a minimized LFR model corresponding to each region that is specified by clicking on the button "Generate LFR systems". The border of the regions becomes green, and newly-created regions will appear in the "dialog box" used by the interpolation method with their names in the following format: "Region (number of region) _interp (dd-mm-yyyy) .mat". It will further be possible to check the quality of the interpolation -- as shown in the Results Section -- by choosing the number of points to be randomly created for interpolation purpose. Whether there are one or more display windows open, these windows can contain a maximum of four graphs. This interface provides a helpful real-time visualization, and it has very good modularity.

A single Graphical User Interface (GUI) that can only be opened from the previous interface was created to facilitate the organization of the data. Indeed, it has been observed that there can be too much information to handle, given the large number of centering and flight points. This GUI classifies state space matrices in the longitudinal or lateral models, centering and flight points. In addition, the flight envelope is generated by providing information on each flight point's trim conditions of the model. "Green" highlighting means that the model is trimmed at this flight point, and "red" highlighting refers to a flight point for which no equilibrium condition was found.

It was possible to accurately develop the Cessna Citation X aircraft's dynamic longitudinal LFR models by means of the state matrix interpolation method using this GUI. The results are very good, and that are further used to study the aircraft's longitudinal eigenvalue stability.

## 5. CONCLUSION

The generation and validation of Cessna Citation X LFR models were automated in this research using a Graphical User Interface (GUI), This GUI generates graphs that represents the aircraft dynamics in its whole envelope for all its uncertainty parameters values, which offered the user a very good visualization tool that facilitated the manipulation of LFRs models, and therefore, it provided a very good understanding of its validation process.

The results provided from the LFR GUI will be used later in Part 2, in the analysis of the longitudinal eigenvalue stability (open loop system without a controller), which will be performed for the 26 interpolated regions.

## ACKNOWLEDGEMENT

This work was performed at the LARCASE (Laboratory of active controls, avionics and aeroservoelasticity research). We would like to thank to the project leader Mr Ken Dustin and his team at CAE Inc. for their support in the development of the Aircraft Research Flight Simulator at the LARCASE laboratory.

This simulator was obtained thanks to research grants that were approved by the Canada Foundation for Innovation (CFI) and the Ministère de Développement de l'Économie, de l'Innovation et de l'Exportation MDEIE. In addition, this research was funded by the Natural Sciences and Engineering Research Council of Canada NSERC in the frame of Canada Research Chair Programs; Dr Ruxandra Botez is Canada Research Chair Holder in Aircraft Modeling and Simulation Technologies. Thanks are also due to Mrs Odette Lacasse and Mr Oscar Carranza at ETS for their continuing enthusiasm and support.

## REFERENCES

[1] C. Fielding, A. Varga, S. Bennani, M. Selier, *Advanced Techniques for Clearance of Flight Control Laws*, Springer Science & Business Media, 2002.

[2] G. Becker, A. Packard, Robust Performance of Linear Parametrically Varying Systems using Parametrically-Dependent Linear Feedback, *Systems & Control Letters*, Vol. **23**, No. 3, pp. 205-215, 1994.

[3] K. Zhou, J. C. Doyle, K. Glover, *Robust and Optimal Control*, New Jersey: Prentice hall Edition, 1996.

[4] W. Zhigang, Y. Chao, A New Approach for Aeroelastic Robust Stability Analysis, *Chinese Journal of Aeronautics*, Vol. **21**, No. 5, pp. 417-422, doi:10.1016/S1000-9361(08)60054-0, 2008.

[5] X. Zhou, L. Liu, Z-j. Chen, H-b. Duan, Validation of Flight Control Law Based on LFT and Structured Singular Value, *Chinese Journal of Aeronautics*, Vol. **20**, No. 1, pp. 60-65. doi:10.1016/S1000-9361(07)60008-9, 2007.

[6] Y. Dai, C. Yang, Methods and Advances in the Study of Aeroelasticity with Uncertainties, *Chinese Journal of Aeronautics*, Vol. **27**, No. 3, pp. 461-474,doi:10.1016/j.cja.2014.04.016, 2014.

[7] D. G. Bates, R. Kureemun, T. Mannchen, Improved Clearance of a Flight Control Law using μ-analysis Techniques, *Journal of Guidance, Control, and Dynamics*, Vol. **26**, No. 6, pp. 869-884, http://dx.doi.org/10.2514/2.6931, 2003.

[8] G. Puyou, Y. Losser, *Clearance Benchmark for a Civil Aircraft, In Optimization Based Clearance of Flight Control Laws*, pp. 11-36, Springer Berlin Heidelberg Edition, 2012.

[9] W. Y. Yan, J. B. Moore, Stable Linear Fractional Transformations with Applications to Stabilization and Multistage H∞ Control Design, *International Journal of Robust and Nonlinear Control*, Vol. **6**, No. 2, pp. 101-122, 1996.

[10] J. C. Cockburn, B. G. Morton, Linear Fractional Representations of Uncertain Systems, *Automatica*, Vol. **33**, No. 7, pp. 1263-1271, 1997.

[11] J. C. Cockburn, *Multidimensional Realizations of Systems with Parametric Uncertainty*, Proceedings of MTNS, Perpignan, France, June 2000.

[12] S. Hecker, A. Varga, Generalized LFT-based Representation of Parametric Uncertain Models, *European Journal of Control*, Vol. **10**, pp. 326-337, 2004.

[13] N. Aouf, B. Boulet. R. M. Botez, H2 and H∞-Optimal Gust Load Alleviation for a Flexible Aircraft, *American Control Conference (ACC) Proceedings*, Chicago, USA7-9 June, Vol. **3**, pp. 1872-1876, 2000.

[14] S. Ibrir, R. M. Botez, Robust Stabilization of Uncertain Aircraft Active Systems, *Journal of Vibration and Control*,Vol. **11**, No. 2, pp. 187-200, 2005.

[15] A. Marcos, J. Veenman, C. Scherer, G. Zaiacomo, D. Mostaza, M. Kerr, H. Köroglu, S. Bennani, Application of LPV Modeling, Design and Analysis Methods to a Re-entry Vehicle, *AIAA Guidance, Navigation and Control Conference Proceedings*, AIAA Paper 2010-8192, 2-5 August, Toronto, Ont., Canada, http://dx.doi.org/10.2514/6.2010-8192, 2010.

[16] Z. Szabó, A. Marcos, D. M. Prieto, M. L. Kerr, G. Rödönyi, J. Bokor, S. Bennani, Development of an Integrated LPV/LFT Framework: Modeling and Data-Based Validation Tool, *IEEE Transactions on Control Systems Technology*,Vol. **19**, No. 1, pp. 104-117, 2011.

[17] A. Varga, G. Looye, D. Moormann, G. Gräbel, Automated Generation of LFT-Based Parametric Uncertainty Descriptions from Generic Aircraft Models, *Mathematical and Computer Modelling of Dynamical Systems*, Vol. **4**, no. 4, pp. 249-274, 1998.

[18] A. Varga, G. Looye, Symbolic and Numerical Software Tools for LFT-Based Low Order Uncertainty Modeling, *Proceedings of the IEEE International Symposium Computer Aided Control System Design*, pp. 1-6, 1999.

[19] J. Tang, C. Wei, W. Meng, Robustness Analysis of Unmanned Helicopter Flight Control Law using μ-analysis Techniques, *6th IEEE Conference on Industrial Electronics and Applications (ICIEA*), 21-23 June 21, pp. 1283-1287, 2011.

[20] S. Dong, Z. Wang, Y. Wang, L. Liu, L. Ou, Tracking Performance Analysis of Flight Control System Based on H-infinity Theory, *International Journal of Modelling, Identification and Control*, Vol. **19**, No. 3, pp. 290-298. doi: 10.1504/IJMIC.2013.055434, 2013.

[21] L. Lei, W. Benli, Multi Objective Robust Active Vibration Control for Flexure jointed struts of Stewart Platforms via H∞ and μ Synthesis, *Chinese Journal of Aeronautics*, Vol. **21**, No. 2, pp. 125-133, doi:10.1016/S1000-9361(08)60016-3, 2008.

[22] A. Varga, A. Hansson, G. Puyou, *Optimization Based Clearance of Flight Control Laws*, Lecture Notes in Control and Information Science, Springer Edition, pp. 121, 2012.

[23] G. Ghazi, R. M. Botez, Development of a High-Fidelity Simulation Model for a Research Environment, *SAE Technical Paper*, 22-24 September, 2015.

[24] G. Ghazi, 2014, *Développement d'une lateforme de simulation et d'un pilote automatique-application aux Cessna Citation X et Hawker 800XP*, Doctoral dissertation, Master's thesis, University of Quebec-École Polytechnique de Montréal, doi: 10.13140/2.1.

[25] Y. Boughari, R. M. Botez, G. Ghazi, F. Theel, Evolutionary Algorithms for Robust Cessna Citation X Flight Control, Paper No. 2014-01-2166, *SAE 2014 Aerospace Systems and Technology Conference*, Cincinnati, Ohio, USA, 2014, September 23-25, doi:10.4271/2014-01-2166.

[26] Y. Boughari, R. M. Botez, G. Ghazi, F. Theel, Flight Control Clearance of the Cessna Citation X using Evolutionary Algorithms, *Proceedings of the Institution of Mechanical Engineers* (*IMechE*), *Part G: Aerospace Engineering*, 2016 Apr. 11, doi: 10.1177/0954410016640821.

[27] Y. Boughari, R. M. Botez, F. Theel et G. Ghazi, *Optimal Flight Control on Cessna Citation X Aircraft Using Differential Evolution*, In IASTED International Conference on Modelling, Identification and Control, MIC. (Innsbruck, Austria, Feb.17-19, 2014), p. 189-198. Coll. Proceedings of the IASTED International Conference on Modelling, Identification and Control: Acta Press. < http://dx.doi.org/10.2316/P.2014.809-052 >, 2014.

[28] Y. Boughari, G. Ghazi, R. M. Botez, F. Theel, New Methodology for Optimal Flight Control Using Differential Evolution Algorithms Applied on the Cessna Citation X Business Aircraft - Part 1. Design and Optimization, *INCAS BULLETIN*, Vol. **9**, Issue 2, (online) ISSN 2247–4528, (print) ISSN 2066–8201, ISSN–L 2066–8201, pp. 31-44, DOI: 10.13111/2066-8201.2017.9.2.3, 2017.

[29] Y. Boughari, G. Ghazi, R. M. Botez, F. Theel, New Methodology for Optimal Flight Control using Differential Evolution Algorithms applied on the Cessna Citation X Business Aircraft - Part 2. Validation on Aircraft Research Flight Level D Simulator, *INCAS BULLETIN*, Vol. **9**, Issue 2, (online) ISSN 2247–4528, (print) ISSN 2066–8201, ISSN–L 2066–8201, pp. 45-59, doi: 10.13111/2066-8201.2017.9.2.4, 2017.

[30] Y. Boughari et al., Optimal Control New Methodologies Validation On the Research Aircraft Flight Simulator of the Cessna Citation X Business Aircaft, *Internationa Journal of Contemporary Energy*, Vol **3**, No. 1, doi: 10.14621/ce.20170102, 2017.

[31] C. Hamel, A. Sassi, R. M. Botez, C. Dartigues, Cessna Citation X Aircraft Global Model Identification from Flight Tests, *SAE International Journal of Aerospace*, Vol. **6**, No. 1, pp. 106-114, doi:10.4271/2013-01-2094, 2013.

[32] C. Hamel, R. M. Botez, M. Ruby, Cessna Citation X Airplane Grey-Box Model Identification without Preliminary Data, *SAE Aerospace Systems and Technology Conference*, Cincinnati, Ohio, USA, 23-25 September, doi: 10.4271/2014-01-2153, 2014.

[33] R. C. Nelson, *Flight Stability and Automatic Control*, McGraw Hill Education, 1998.

[34] A. Garulli, A. Masi, S. Paoletti, E. Turkoglu, *LFR_RAI User's Guide*, March 3, pp. 1-28, available at http://www.dii.unisi.it/~garulli/lfr_rai.

[35] C. Poussot-Vassal, C. Roos, Generation of a Reduced-Order LPV/LFT Model from a set of Large-Scale MIMO LTI Flexible Aircraft Models, *Control Engineering Practice*, September 30, Vol. **20**, No. 9, pp. 919-930, 2012.

[36] S. Hecker, A. Varga, J. F. Magni, *Enhanced LFR-toolbox for MATLAB*, *Computer Aided Control Systems Design*, IEEE International Symposium on Computer Aided Control Systems Design, September 4, pp. 25-29, 2004.